Radiative decays of B_c mesons in a Bethe-Salpeter model

A. Abd El-Hady,[1,*] J. R. Spence,[2] and J. P. Vary[2]

[1]*Physics Department, King Khalid University, Abha 9004, Saudi Arabia*

[2]*Department of Physics and Astronomy, Iowa State University, Ames, Iowa 50011, USA*

(Received 6 December 2004; published 3 February 2005)

We evaluate the complete spectrum of the B_c mesons, below the open flavor BD threshold, in a Bethe-Salpeter model. We make predictions for the radiative decay widths of the B_c excited states. We compare our results with those of other models.

DOI: 10.1103/PhysRevD.71.034006 PACS numbers: 13.20.He, 11.10.St, 13.20.−v

I. INTRODUCTION

The B_c meson discovered by the CDF collaboration [1] in $p\bar{p}$ collisions at $\sqrt{s} = 1.8$ TeV completes the family of mixed flavor mesons. The B_c meson has a $\bar{b}$ antiquark and a c quark. Current and future experiments at the Tevatron and LHC are expected to provide large samples of the excited states of the B_c mesons [2]. This will make possible the study of the spectroscopy and the decays of the B_c mesons. The B_c meson family lies intermediate in mass and size between the $\bar{c}c$ (J/ψ) and the $\bar{b}b$ (Υ) families where the heavy quark interactions are believed to be understood rather well. Comparison between experimental measurement and theoretical results will improve our understanding of these interactions and guide us in the search for multiquark and molecular exotics such as the recently claimed (discovered) D_{sJ} [3–5] and $X(3872)$ [6].

Different models [7–12] including various versions of potential models and QCD sum rules have been used to evaluate the B_c spectrum yielding results consistent with the experimentally measured ground state mass and lifetime. The B_c mesons have nonvanishing flavor quantum numbers which are conserved in strong and electromagnetic interactions. Therefore, the B_c states, below the open flavor BD threshold, can only decay weakly or radiatively. These states are expected to be relatively long-lived and easier to be observed experimentally. From the theoretical side, weak and radiative decays are free from uncertainties encountered in strong decays which makes the decays of these states theoretically more tractable.

In a previous paper [13], we have evaluated a limited set of the B_c spectrum using a model based on reductions of the Bethe-Salpeter equation (BSE). We have used a set of parameters fixed from previous investigations of other meson spectra. Our results agreed very well with the experimentally measured ground state mass and lifetime. We also evaluated the B_c decay constant, the $\bar{b}$ antiquark and the c quark inclusive decay widths and the weak annihilation width.

We also evaluated the exclusive semileptonic $[B_c \to P(V)e\nu]$ and two-body nonleptonic $(B_c \to PP, PV, VV)$ decay widths [14], where P (V) denotes a pseudoscalar (vector) meson. We used the BSE amplitudes to evaluate the semileptonic form factors and used factorization to obtain the nonleptonic decay widths in terms of the semileptonic form factors and the weak decay constants.

In the present paper, we evaluate the complete B_c spectrum below the open flavor BD threshold and consider the radiative $E1$ and $M1$ electromagnetic transitions. This complements our picture [13,14] of the B_c mesons. Radiative decays are the dominant decay modes of the B_c excited states having widths of about a fraction of MeV, much greater than the weak widths at the order of meV. Therefore, accurate determination of the masses and the radiative decay widths will be extremely important for understanding the B_c spectrum and distinguishing exotic states.

The paper is organized as follows. In the next section we briefly outline our model and compare our spectrum with those of other models. We then evaluate the $E1$ and $M1$ radiative decays. Finally we discuss our results.

II. MODEL AND SPECTROSCOPY

We applied a relativistic model based on reductions of the BSE to evaluate the B_c spectrum. The BSE is a suitable starting point for treating hadrons as relativistic bound states of quarks and antiquarks, just as the Dirac equation provides a relativistic description of a fermion in an external field. The BSE for a bound state may be written in momentum space in the form [15]

$$G^{-1}(P, p)\psi(P, p) = \int \frac{1}{(2\pi)^4} V(P, p - p')\psi(P, p')d^4p'. \tag{1}$$

Where P is the four-momentum of the bound state, p is the relative four-momentum of the constituents. The BSE has three elements, the two particle propagator (G) and the interaction kernel (V) which we provide as input, and the amplitude (ψ) obtained by solving the equation. We also solve for the energy, which is contained in the propagator. We used a reduction of the BSE where the two particle

*Permanent address: Physics Department, Faculty of Science, Zagazig University, Zagazig, Egypt.

propagator is modified in a way that keeps covariance and reduces the four-dimensional BSE into a three-dimensional equation [16]. We considered an interactional kernel that consists of two terms, one for the short range one gluon exchange V_{OGE} and the other for the long range phenomenological confinement interaction V_{CON} [17].

$$V_{OGE} + V_{CON} = -\frac{4}{3}\alpha_s \frac{\gamma_\mu \otimes \gamma_\mu}{(p-p')^2} + \sigma \lim_{\mu\to 0} \frac{\partial^2}{\partial \mu^2} \times \frac{\mathbf{1}\otimes\mathbf{1}}{-(p-p')^2+\mu^2}. \quad (2)$$

Here, α_s is the strong coupling, which is weighted by the meson color factor of $\frac{4}{3}$, and the string tension σ is the strength of the confining part of the interaction. While the one gluon exchange V_{OGE} has the vector nature, we adopt a scalar Lorentz structure for V_{CON} as discussed in [16]. We solve for the energies and the amplitudes in momentum space and transform these amplitudes into coordinate space.

We have included seven parameters in our model, four masses ($m_u = m_d, m_s, m_c, m_b$), two parameters to fix the strong coupling α_s and control its running with the meson mass, and the last parameter is the string tension σ of the confining interaction. We fixed the parameters of our model by fitting the spectra of other mesons as described in [17]. We obtained a good fit for a wide range of meson masses with root mean square deviation from experimental masses of about 50 MeV.

Table I compares the parameters relevant to the B_c mesons of our model with those of different models in the literature. In Table I, m_c and m_b are the masses of the c and b quark, respectively, while α_s is the strong coupling of the one gluon exchange and σ is the string tension of the confining interaction. In many models, including ours, α_s runs with the meson mass, thus Table I gives α_s at the scale of the ground state mass of the B_c mesons. The model used in [8] employs the Martin potential [18] which is not linear but varies with powers of the quark antiquark distance.

We notice that our m_c and m_b values are smaller than those of other models, while our string tension σ is larger. The values of the strong coupling α_s are consistent around 0.36 except in [11] where α_s is 0.265 and in [12] where α_s is 0.21.

Figure 1 shows the B_c spectrum of our model. The horizontal dashed line represents the BD threshold (7143 MeV). States above the BD threshold can decay strongly into two heavy-light mesons while those below that line can only decay weakly or radiatively. Our result for the B_c ground state mass (6.380 GeV/c^2) agrees very well with the Experimental result of the CDF collaboration $6.40 \pm 0.39(\text{stat}) \pm 0.13(\text{syst})$ GeV/c^2 [1].

TABLE I. The parameters of different models relevant to the B_c mesons.

	This work	EQ [7]	GKLT [8]	EFG [11]	GI [12]
m_c (GeV)	1.39	1.48	1.8	1.55	1.628
m_b (GeV)	4.68	4.88	5.174	4.88	4.977
α_s	0.357	0.361	0.391	0.265	0.21
σ (GeV^2)	0.211	0.16	⋯	0.18	0.18

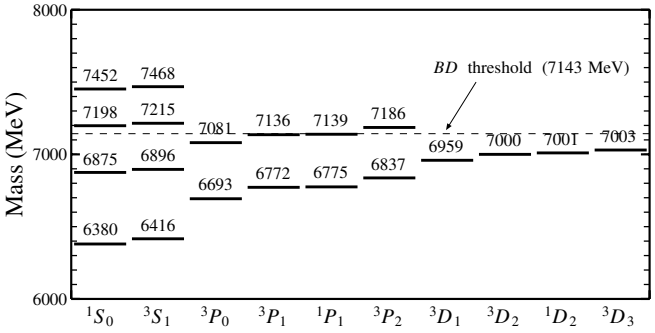

FIG. 1. The B_c mass spectrum.

Table II compares our B_c spectrum with those of some other models. One may notice that the hyperfine splitting of our model ($^3S_1 - {}^1S_0$ difference) is smaller than those of other models, while the fine splitting of the P states is larger in our model. We treat the interactions responsible for these splittings directly in the bound state problem while Eichten and Quigg [7], for example, treat them perturbatively. Experimental results for the excited states of the B_c mesons are needed to clarify these differences and improve our knowledge of the parameters shown in Table I.

TABLE II. B_c spectrum in units of GeV.

Level	This work	EQ [7]	GLKT [8]	EFG [11]	GI [12]
1^1S_0	6.380	6.264	6.253	6.270	6.271
1^3S_1	6.416	6.337	6.317	6.332	6.338
1^3P_0	6.693	6.700	6.683	6.699	6.706
1^3P_1	6.772	6.730	6.717	6.734	6.741
1^1P_1	6.775	6.736	6.729	6.749	6.750
1^3P_2	6.837	6.747	6.743	6.762	6.768
2^1S_0	6.875	6.856	6.867	6.835	6.855
2^3S_1	6.896	6.899	6.902	6.881	6.887
1^3D_1	6.959	7.012	7.008	7.072	7.028
1^3D_2	7.000	7.012	7.001	7.077	7.041
1^1D_2	7.001	7.009	7.016	7.079	7.036
1^3D_3	7.003	7.005	7.007	7.081	7.045
2^3P_0	7.081	7.108	7.088	7.091	7.122
2^3P_1	7.136	7.135	7.113	7.126	7.145
2^1P_1	7.139	7.142	7.124	7.145	7.150
2^3P_2	7.186	7.153	7.134	7.156	7.164
3^1S_0	7.198	7.244	⋯	7.193	7.250
3^3S_1	7.215	7.280	⋯	7.235	7.272
4^1S_0	7.452	7.562	⋯	⋯	7.572
4^3S_1	7.468	7.594	⋯	⋯	7.588

We note that the lifetime of the B_c ground state as reported by CDF is $0.46^{+0.18}_{-0.16}(\text{stat}) \pm 0.03(\text{syst})$ ps [1] corresponding to a width of about 1.43 meV. Three different processes contribute to the B_c ground state width: inclusive $\bar{b}$ decays, inclusive c decays and $\bar{b}$-c annihilation. For excited B_c states the corresponding weak decays will have partial widths similar to or less than the ground state widths (since the weak $\bar{b}$-c annihilation will be forbidden for $S \neq 0$ states). Radiative decays having widths of the order of a fraction of MeV (as evaluated in the next section) will be the dominant decay modes of the B_c excited states.

Using the B_c spectrum and the BSE amplitudes in momentum space or the transformed coordinate space amplitudes one can evaluate the radiative transition widths between the B_c states. This is what we address in the next section.

III. RADIATIVE DECAYS

The electromagnetic radiative decays of the B_c mesons are of the electric dipole ($E1$) and the magnetic dipole ($M1$) types. The $E1$ partial decay widths can be written as [7,19,20]

TABLE III. Comparison of the results for the $E1$ transition rates of the B_c mesons. The columns labeled (This work) present our results.

Transition	ω (MeV)		$\lvert\langle f\rvert r\rvert i\rangle\rvert$ (GeV^{-1})		$\Gamma(i \to f + \gamma)$ (keV)	
	This work	EQ [7]	This work	EQ [7]	This work	EQ [7]
$1^3P_2 \to 1^3S_1 + \gamma$	408	397	1.613	1.714	109.8	112.6
$1^3P_1 \to 1^3S_1 + \gamma$	347	382	1.619	1.714	67.8	99.5
$1^3P_1 \to 1^1S_0 + \gamma$	381	450	1.537	1.714	0.0	0.0
$1^1P_1 \to 1^3S_1 + \gamma$	349	387	1.615	1.714	0.0	0.1
$1^1P_1 \to 1^1S_0 + \gamma$	383	455	1.531	1.714	81.8	56.4
$1^3P_0 \to 1^3S_1 + \gamma$	270	353	1.617	1.714	32.1	79.2
$2^3S_1 \to 1^3P_2 + \gamma$	58	151	1.870	2.247	0.7	17.7
$2^3S_1 \to 1^3P_1 + \gamma$	123	167	1.836	2.247	3.9	14.5
$2^3S_1 \to 1^1P_1 + \gamma$	120	161	1.887	2.247	0.0	0.0
$2^3S_1 \to 1^3P_0 + \gamma$	200	196	1.862	2.247	5.8	7.8
$2^1S_0 \to 1^3P_1 + \gamma$	102	125	1.915	2.247	0.0	0.0
$2^1S_0 \to 1^1P_1 + \gamma$	99	119	1.965	2.247	7.1	5.2
$1^3D_3 \to 1^3P_2 + \gamma$	163	258	2.404	2.805	18.7	98.7
$1^3D_2 \to 1^3P_2 + \gamma$	160	258	2.405	2.805	4.4	24.7
$1^3D_2 \to 1^3P_1 + \gamma$	224	274	2.395	2.805	35.8	88.8
$1^3D_2 \to 1^1P_1 + \gamma$	221	268	2.436	2.805	0.0	0.1
$1^3D_1 \to 1^3P_2 + \gamma$	121	258	2.431	2.805	0.2	2.7
$1^3D_1 \to 1^3P_1 + \gamma$	184	274	2.415	2.805	11.4	49.3
$1^3D_1 \to 1^1P_1 + \gamma$	182	268	2.454	2.805	0.0	0.0
$1^3D_1 \to 1^3P_0 + \gamma$	262	302	2.434	2.805	43.9	88.6
$1^1D_2 \to 1^1P_1 + \gamma$	222	268	2.433	2.805	120.8	92.5
$2^3P_2 \to 1^3S_1 + \gamma$	729	770	0.194	0.304	9.1	25.8
$2^3P_2 \to 2^3S_1 + \gamma$	285	249	2.525	2.792	91.3	73.8
$2^3P_2 \to 1^3D_3 + \gamma$	181	142	2.249	2.455	31.5	17.8
$2^3P_2 \to 1^3D_2 + \gamma$	184	142	2.238	2.455	5.8	3.2
$2^3P_2 \to 1^3D_1 + \gamma$	223	142	2.046	2.455	0.6	0.2
$2^3P_1 \to 1^3S_1 + \gamma$	684	754	0.178	0.304	6.3	22.1
$2^3P_1 \to 2^3S_1 + \gamma$	236	232	2.553	2.792	53.5	54.3
$2^3P_1 \to 1^3D_2 + \gamma$	136	125	2.277	2.455	12.0	9.8
$2^3P_1 \to 1^3D_1 + \gamma$	175	125	2.078	2.455	7.2	0.3
$2^1P_1 \to 1^3S_1 + \gamma$	686	760	0.209	0.304	0.0	2.1
$2^1P_1 \to 2^3S_1 + \gamma$	239	239	2.509	2.792	0.0	5.4
$2^1P_1 \to 1^3D_2 + \gamma$	138	131	2.232	2.455	0.0	11.5
$2^1P_1 \to 1^3D_1 + \gamma$	177	131	2.029	2.455	0.0	0.4
$2^3P_0 \to 1^3S_1 + \gamma$	634	729	0.193	0.304	5.9	21.9
$2^3P_0 \to 2^3S_1 + \gamma$	183	205	2.531	2.792	24.3	41.2
$2^3P_0 \to 1^3D_1 + \gamma$	121	98	2.053	2.455	9.3	6.9

TABLE IV. Comparison of the results for the $E1$ transition rates of the S-wave B_c mesons. The columns labeled (This work) present our results.

Transition	ω (MeV)		$\lvert\langle f\rvert j_0(kr/2)\lvert i\rangle\rvert$		$\Gamma(i \to f + \gamma)$ (keV)	
	This work	EQ [7]	This work	EQ [7]	This work	EQ [7]
$2^3S_1 \to 2^1S_0 + \gamma$	21	43	0.9949	0.9990	0.0037	0.0289
$2^3S_1 \to 1^1S_0 + \gamma$	496	606	0.0523	0.0395	0.1357	0.1234
$2^1S_0 \to 1^3S_1 + \gamma$	443	499	0.0393	0.0265	0.1638	0.0933
$1^3S_1 \to 1^1S_0 + \gamma$	36	72	0.9979	0.9993	0.0189	0.1345

$$\Gamma_{E1}(i \to f + \gamma) = \frac{4\alpha\langle e_Q\rangle^2}{3}(2J_f + 1)\omega^3|\langle f|r|i\rangle|^2 C_{fi} \quad (3)$$

where the mean charge is

$$\langle e_Q\rangle = \frac{m_b e_c - m_c e_{\bar{b}}}{m_b + m_c}, \quad (4)$$

$e_c = 2/3$ is the c quark charge and $e_{\bar{b}} = 1/3$ is the charge of the $\bar{b}$ antiquark in units of $|e|$, α is the electromagnetic fine structure constant, ω is the photon energy

$$\omega = \frac{M_i^2 - M_f^2}{2M_i^2} \quad (5)$$

and the statistical factor C_{fi} is given by ($S = S_i = S_f$)

$$C_{fi} = \max(L_i, L_f)\begin{Bmatrix} L_f & J_f & S \\ J_i & L_i & 1 \end{Bmatrix}^2. \quad (6)$$

The mean charge expresses the fact that the emitted γ can be attached to the c quark or the $\bar{b}$ antiquark. The lighter c quark is more efficient in this process. The statistical factor C_{fi} results from the angular momentum coupling. Table III compares our results (This work) and the results of Eichten and Quigg (EQ) [7] for the transition energy (in MeV), the transition matrix element $|\langle f|r|i\rangle|$ (in GeV^{-1}), and the transition width (in keV). We notice that the transition energies may differ by a factor of about 2 while the transition matrix element are very close to each other. The transition matrix elements in our model depends on the initial and final values of L, J, S since our model treats the spin-orbit, the spin-spin, and the tensor interactions in the bound state problem while the transition matrix elements of Eichten and Quigg [7] depend on the initial and final L only since they take care of these splittings perturbatively.

The $M1$ partial decay widths between the S-wave states can be written as [7,19,20]

$$\Gamma_{M1}(i \to f + \gamma) = \frac{16\alpha\mu^2}{3}(2J_f + 1)\omega^3|\langle f|j_0(kr/2)|i\rangle|^2, \quad (7)$$

where the magnetic dipole moment is

$$\mu = \frac{m_b e_c - m_c e_{\bar{b}}}{4m_c m_b}. \quad (8)$$

Allowed $M1$ transitions correspond to triplet-singlet transitions between S-wave states of the same n quantum number, while hindered $M1$ transitions are either triplet-singlet or singlet-triplet transitions between S-wave states of different n quantum numbers. In the nonrelativistic limit these hindered transitions are suppressed by wave function orthogonality. Taking relativistic effects in the wave function (in addition to the large ω^3 dependence of the width) makes the widths of these transitions comparable with the widths of the allowed ones. Table IV compares our results (This work) and the results of Eichten and Quigg (EQ) [7] for the transition energy (in MeV), the transition matrix element $|\langle f|j_0(kr/2)|i\rangle|$, and the transition width (in keV).

Table IV shows differences between the transition energies (spin-spin splittings), while the transition matrix elements are comparable. It also shows that hindered transitions have widths at the same level as the allowed ones.

IV. SUMMARY

We have evaluated the B_c spectrum below the BD threshold using a reduction of the BSE. We have made predictions for the transition rates of the $E1$ and $M1$ radiative decays. We compared our results with the results of other models in the literature. Experimental results will help clarify the spin-spin and spin-orbit splittings of different models and consequently improve our knowledge of physical quantities such as the quark masses and the strong coupling α_s at the scale of M_{B_c}. Measurements of radiative transitions and comparison with such results may indicate the existence of exotic multiquark or molecular exotics.

ACKNOWLEDGMENTS

This work was supported in part by the U.S. Department of Energy, Grant No. DE-FG02-87ER40371, Division of Nuclear Physics.

[1] CDF Collaboration, F. Abe *et al.*, Phys. Rev. D **58**, 112004 (1998).
[2] E. Braaten, S. Fleming, and T. C. Yuan, Annu. Rev. Nucl. Part. Sci. **46**, 197 (1996).
[3] BABAR Collaboration, B. Aubert *et al.*, Phys. Rev. Lett. **90**, 242001 (2003).
[4] CLEO Collaboration, D. Besson *et al.*, Phys. Rev. D **68**, 032002 (2003).
[5] Belle Collaboration, P. Krokovny *et al.*, Phys. Rev. Lett. **91**, 262002 (2003).
[6] Belle Collaboration, S. K. Choi *et al.*, Phys. Rev. Lett. **91**, 262001 (2003).
[7] E. Eichten and C. Quigg, Phys. Rev. D **49**, 5845 (1994).
[8] S. S. Gershtein, V. V. Kiselev, A. K. Likhoded, and A. V. Tkabladze, Phys. Usp. **38**, 1 (1995); V. V. Kiselev, A. K. Likhoded, and A. V. Tkabladze, Phys. Rev. D **51**, 3613 (1995); S. S. Gershtein, V. V. Kiselev, A. K. Likhoded, A. V. Tkabladze, A. V. Berezhnoi, and A. I. Onishchenko, hep-ph/9803433.
[9] S. N. Gupta and J. M. Johnson, Phys. Rev. D **53**, 312 (1996).
[10] L. P. Fulcher, Phys. Rev. D **60**, 074006 (1999).
[11] D. Ebert, R. N. Faustov, and V. O. Galkin, Phys. Rev. D **67**, 014027 (2003).
[12] S. Godfrey, Phys. Rev. D **70**, 054017 (2004); S. Godfrey and N. Isgur, Phys. Rev. D **32**, 189 (1985).
[13] A. Abd El-Hady, M. A. K. Lodhi, and J. P. Vary, Phys. Rev. D **59**, 094001 (1999).
[14] A. Abd El-Hady, J. H. Muñoz, and J. P. Vary, Phys. Rev. D **62**, 014019 (2000).
[15] C. Itzykson, and J. B. Zuber, *Quantum Field Theory* (McGraw-Hill, New York, 1980) (Chap. 10 gives a review of Bethe-Salpeter equation).
[16] A. J. Sommerer, J. R. Spence, and J. P. Vary, Phys. Rev. C **49**, 513 (1994), and references therein.
[17] Alan J. Sommerer, A. Abd El-Hady, John R. Spence, and James P. Vary, Phys. Lett. B **348**, 277 (1995).
[18] A. Martin, Phys. Lett. **93B**, 338 (1980).
[19] E. Eichten, K. Gottfried, T. Kinoshita, K. D. Lane, and T. M. Yan, Phys. Rev. D **17**, 3090 (1978); **21**, 313(E) (1980).
[20] E. Eichten and K. Gottfried, Phys. Lett. **66B**, 286 (1977).